

# The absolute Frequency measurement of atomic thallium $6P_{1/2} \rightarrow 7S_{1/2}$ transition using optical frequency comb

Yi-Wei Liu,\* Yu-Hung Lien, Wei-Ling Cheng, Chia-Hui Ho, and Jow-Tsong Shy  
*Department of Physics, National Tsing Hua University, Hsinchu 300, Taiwan*

Hsiang-Chen Chui  
*Department of Electrical Engineering, National Tsing Hua University, Hsinchu 300, Taiwan*  
(Dated: February 5, 2020)

The Doppler-free spectroscopy of atomic thallium ( $^{203}\text{Tl}$  and  $^{205}\text{Tl}$ )  $6P_{1/2} \rightarrow 7S_{1/2}$  transitions have been observed using two counter-propagating laser beams perpendicular to the atomic beam, and the absolute frequencies of these transitions have been measured to an accuracy of  $<1$  MHz (1 ppb) using optical frequency comb. The hyperfine splittings derived from our results were improved by a factor of 7~8. The isotope shifts are in agreement with the previous experimental results.

PACS numbers: 32.10.Fn, 31.30.Gs, 27.80.+w

## I. INTRODUCTION

High precision measurement in atomic system shows very promising in testing new physics beyond the standard model. The linear stark effect measurement in atomic thallium sets the current upper limit of electrons electrical dipole moment (EDM)[1], whose existence implies the CP violation. Meanwhile, atomic thallium also plays an important role in parity non-conservation (PNC) experiment. The PNC effect has been observed in atomic thallium system using  $6P_{1/2} \rightarrow 6P_{3/2}$  transition in 1995 [2, 3]. The optical rotation measurement of thallium reached 1% of experimental uncertainty. Combining the theoretical calculation, it leads to the weak charge of thallium nucleus, which can be compared with the predication of the standard model. However, the dominating uncertainty is the theoretical calculation, which is as large as 3%. Such a large uncertainty is due to complicate atomic structure. In comparison with the most recent PNC experiment with cesium, whose atomic structure is better understood, an experimental accuracy of 0.5% has been achieved, and the accuracy of theoretical calculation is only 1% [4, 5, 6]. This result leads to the most accurate measurement of the weak charge of the cesium nucleus.

In atomic thallium, strong correlation between three valance-electrons can not be treated accurately using many-body-perturbation theory (MBPT), which is the only calculation needed to be included in the case of cesium, as pointed out by Kozlov [7] and Dzuba [8]. The calculation combining MBPT and the configuration interaction (CI) [8] was developed to solve the correlation problem. To test the accuracy of this theoretical approach, various observables, such as transition energies, hyperfine splittings, transition amplitudes, and polarizabilites, should be calculated and compared with exper-

imental results. Therefore, experimental measurements with high precision would be important for the improvement of theoretical calculation.

In this paper we report precision measurements of atomic thallium  $6P_{1/2} \rightarrow 7S_{1/2}$  transition frequency and isotope shifts using optical frequency comb(OFC), which is a versatile optical frequency measuring tool [9]. The absolute frequencies in the region between 500-1000 nm can be measured to high accuracies with OFC. A self-referenced Ti:Sapphire frequency comb linked to a master atomic clock can reach to an accuracy of kHz, or better. Such a high precision experiment was possible only using a complicate frequency chain. Now, in most of cases with a compact OFC system, the accuracy of optical transition frequency measurement is only limited by the linewidth of the observed atomic or molecular transitions and signal-to-noise ratio of the spectrum, rather than the frequency measuring tool itself.

In atomic thallium, the ground state 378 nm resonance transition has been studied in details using both gas cell [10] [11] and atomic beam [12]. However, the large linewidths, due to laser or the Doppler broadened features, limited the accuracy of measurements. The Doppler-broadened spectrum of this transition has been performed in both of direct absorption [10] and fluorescence [11] experiments with a gas cell. However, to our knowledge, no Doppler-free saturation spectroscopy has been observed yet. Hence, the large Doppler linewidth (600 MHz) limits the accuracy of isotope shift and hyperfine splitting measurement in  $7S_{1/2}$ .

The major difficulty of the cell experiment to acquire Doppler-free spectrum is due to the large branch ratio of  $7S_{1/2} \rightarrow 6P_{3/2}$  decay route (in comparison with  $7S_{1/2} \rightarrow 6P_{1/2}$ , see Fig. 1), and the long lifetime of  $6P_{3/2}$  metastable state. The exciting 378 nm laser causes an optical pumping effect to trap population in the  $6P_{3/2}$  metastable state, then a long recovering time of the  $6P_{1/2}$  ground state population. This implies a low effective saturation intensity of  $6P_{1/2} \rightarrow 7S_{1/2}$  transition, therefore a strong power broadening effect. To perform

\*Electronic address: ywliu@phys.nthu.edu.tw

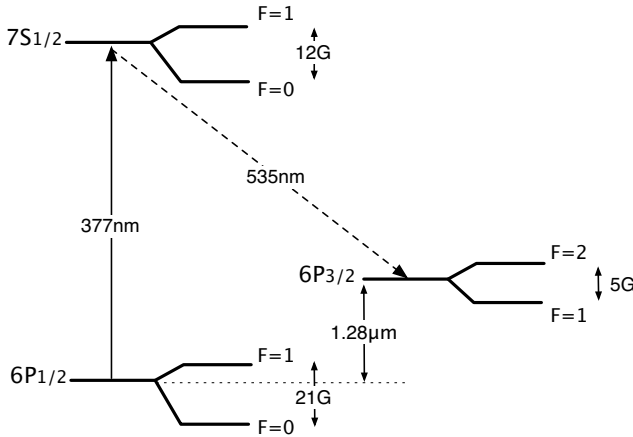


FIG. 1: The partial level diagram of atomic thallium (not scaled).

the Doppler-free saturation spectroscopy with gas cell, even the minimum required power for reasonable signal strength could induce a large power-broadened linewidth close to Doppler width. Lowering laser intensity will not reduce power broadening only, but also the signal strength. A detailed study of such optical pumping effect in atomic thallium can be found in [11].

In the atomic beam experiment, the finite laser-atom interaction time (transit time) becomes an effective shorter recover time of ground state population [13], and then reduces power broadening. Although, there is a trade-off of transit time broadening. In the interaction region of 1 mm, the transit time broadening of atom with a velocity of 300 m/s, is  $< 1$  MHz. Using atomic beam spectroscopy with only one single laser beam, the Doppler shift becomes a serious systematic error, because of the imperfect perpendicular between laser and atomic beam. In our experiment, we employed two counter propagating laser beams and observed the Lamb dip to eliminate such a problem. The observed linewidth of Doppler-free spectrum is only  $\sim 20$  MHz without the first order Doppler shift.

## II. EXPERIMENT

The experimental setup is illustrated as Fig. 2. A collimated atomic beam was irradiated perpendicularly by the frequency-doubled 755 nm Ti:sapphire. The atomic beam source was an effusion oven containing thallium. The transition was detected by measuring 535 nm fluorescence. A small portion of 755 nm laser beam was picked up using a blank glass plate, and sent to optical frequency comb through a single mode optical fiber. A reference cavity with a FSR=300 MHz was used to monitor the laser mode while laser was scanning. The absolute frequency of laser was also measured using a home-made wavemeter with GHz accuracy.

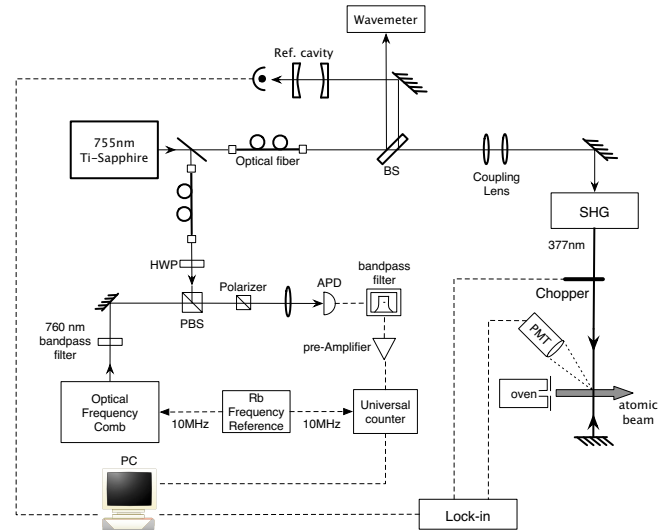


FIG. 2: The experimental setup of absolute frequency measurement of thallium  $6P_{1/2} \rightarrow 7S_{1/2}$  transition

### A. 378 nm Laser System

The 378 nm UV light was generated using a LBO crystal (Breswter's angle cut,  $3 \times 3 \times 10$  mm $^3$ ) in a enhance cavity pumped by a Ti:sapphire laser (Coherent MBR-110) of 755 nm. The enhance cavity was a ring configuration with astigmatism compensation. Cavity resonance was locked on the fundamental laser frequency using the technique of polarization rotation [14]. The typical conversion efficiency was 15%/W with an input coupler of T=3%. 500  $\mu$ W was used in our experiment. The intensity noise was  $< 5\%$  due to the acoustic vibration in the frequency of  $\sim$  kHz. It was collimated to a beam size of 3 mm  $\times$  10 mm using an AR coated lens. The longer side of the elliptical beam shape was parallel to the atomic beam.

### B. Atomic Beam and Signal Detection

The collimated atomic beam with reduced transverse velocity component was used to reduce the Doppler broadening effect and to increase the spectral resolution. The thermal atomic beam, as in Fig. 3, was generated from thallium bulk, which was heated to 450°C. The temperature near the front exit hole was kept 50° higher than the rest part of oven to prevent condensation using another heater. The most probable velocity of thallium atom was  $\sim 300$  m/s. The atomic thallium beam was collimated using two 2 mm apertures separated by 5 mm. The residual Doppler width, due to the beam divergence, was estimated to be 30 MHz in our system. These apertures, between oven and experimental chambers, were also for differential pumping. The experimental chamber was pumped using a small turbo pump (50 l/s) to maintain a pressure  $< 10^{-5}$  torr. The oven cham-

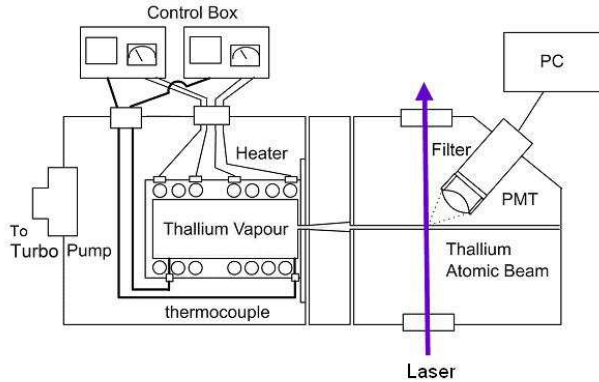


FIG. 3: The atomic beam apparatus.

ber was pumped using a larger turbo (170 l/s) to reach a pressure  $\sim 10^{-5}$  torr. The higher pressure of this was caused by the high temperature of oven. The flange joining these two chambers was water-cooled to prevent heat-transferring from oven to experimental chamber.

Two counter-propagating laser beams were used to eliminate the linear Doppler shift, since the resulted shifts of counter-propagating directions are opposite and the Lamb dip can be observed. Two view ports for laser injection are AR coated UV fused silica. Laser induced fluorescence (LIF) was collected using a 1 inch  $f=30$ mm lens, passed through a dielectric 535 nm filter, and detected using a photomultiplier. The laser intensity was modulated using an optical chopper with a frequency of 2 kHz to reduce noise.

### C. Optical Frequency Comb

The optical frequency comb system was based on a mode-locked Ti:Sapphire laser (Giga Jet 20) with 1 GHz repetition rate, and pumped by 5W 532 nm DPSS Laser (Millennia V). It was a self-reference configuration linked to a rubidium clock (SRS PRS10) using the technique of optical frequency synthesizer [9], as shown in Fig. 4. All of the electronic universal counters and the frequency synthesizer were externally referenced to the same rubidium frequency standard. A 760 nm bandpass filter was used to filter out the unnecessary frequency comb lines and to avoid optical damage of the photodiode (Fig. 2). The frequency fluctuation of the stabilized repetition frequency and offset frequency were 4 mHz, and 11 mHz, respectively. The total frequency fluctuation is few kHz in optical frequency ( $N = 4 \times 10^5$ ), and the accuracy, which was limited by the rubidium master clock and phase noise from frequency synthesizer, was  $10^{-11}$  [15]. The Allen deviation of stabilized repetition rate is shown in Fig. 5. It could be improved by linking the master clock to 1pps signal from GPS receiver. However, This is not necessary in our experiment, since the required accuracy is few tens kHz.

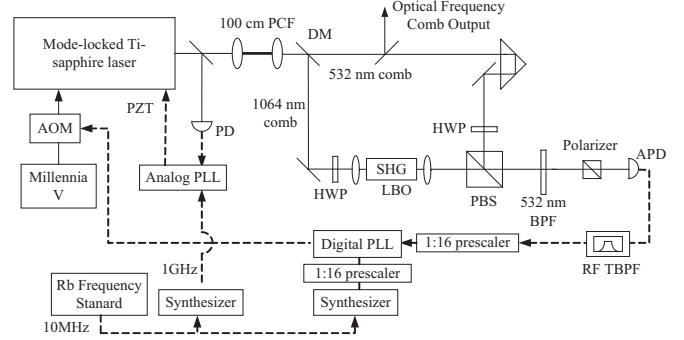


FIG. 4: The self-reference optical frequency comb with a mode-locked Ti:Sapphire laser and a 100 cm photonic crystal fiber.

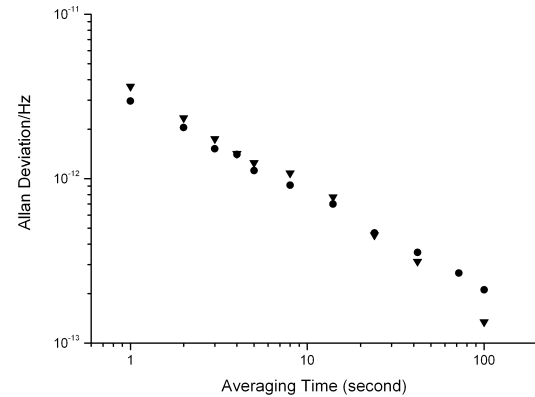


FIG. 5: The Allan deviation of repetition rate (circle) and 1 GHz frequency from HP8643A frequency synthesizer (triangle).

We calibrated this frequency comb system by measuring the well-known  $a_{10}$  hyperfine component of molecular iodine R(56)32-0 transition at 532 nm. The result is in good agreement with the established international standard.

### D. Frequency measurement

The 755 nm laser and frequency comb laser were combined using a polarization beam splitter (PBS), and projected to  $45^\circ$  polarization using a polarizer. The beat frequency, which was detected using an avalanche photodiode (APD), and the fluorescence signal were simultaneously recorded by a computer. We performed a very slow scan, which is 100 MHz/min, to minimize the lag between the frequency reading and fluorescence signal output. Although such a lag effect was cancelled out by backward scanning. A single scan consists of 1000–2000 data points within the frequency range of 100–200 MHz in terms of laser frequency.

The laser frequency can be calculated with a simple equation :

$$f_{\text{unknown}} = N \times f_r \pm f_o \pm f_b ,$$

where the repetition rate of comb laser  $f_r$  is  $\sim 1$  GHz.  $N$  was a large integer,  $\sim 4 \times 10^5$ . The offset frequency of comb laser  $f_o$  and the measured beat frequency  $f_b$  were typically several hundreds MHz. Firstly,  $N$  was roughly determined by the home-made wavemeter with an accuracy of GHz. Then, comparing several scans of the same transition with various  $f_o$ , a series of corresponding measurements of  $f_b$  was obtained. Since each set of  $f_o$ ,  $f_b$ , and  $N$  should result in the same frequency, the signs of  $f_o$  and  $f_b$ , and  $N$  can be accurately determined. To improve the statistic accuracy, the final spectrum was a histogram combining several different scans. The error-bar of the histogram was given by the standard deviation of signal strength of the same laser frequency bin. Figure 6 shows the histogram of all (20) measurements of  $^{203}\text{Tl}$ :  $6P_{1/2}(F=0) \rightarrow 7S_{1/2}(F=1)$  transition. The binning of frequency is 0.5 MHz. Using 0.1 MHz binning, there was no improvement or degradation of the resulted transition frequency.

The spectrum was fitted to a combination of two Viogt and a Lorentzian functions:

$$\begin{aligned} S = & A_1 \times \text{Voigt}(\omega_0 - \omega_{\text{shift}}, \text{WL}, \text{WG1}) \\ & + A_2 \times \text{Voigt}(\omega_0 + \omega_{\text{shift}}, \text{WL}, \text{WG2}) \\ & - A_3 \times \text{Lorentzian}(\omega_0, \text{WL}) \\ & + C \end{aligned} \quad (1)$$

The negative sign of  $A_3$  represents the central dip of the spectrum.  $\text{WG1}$  and  $\text{WG2}$  are the Gaussian widths of two Voigt functions.  $\text{WL}$  is the homogenous broadening, including laser linewidth, transit time broadening, power broadening, natural linewidth, and so forth. Two Viogt functions refer to two fluorescence signals excited from two counter-propagating light. The splitting of these two profiles ( $\omega_{\text{shift}}$ ) is due to that the laser beam is not exactly perpendicular to the atomic beam ( $\Delta\phi$ ). In our experiment,  $\omega_{\text{shift}} \sim 15$  MHz and  $\Delta\phi \sim 38$  mrd, which is consistent with our experimental setup. We scanned  $\Delta\phi$  from +40 mrd to -40 mrd to confirm that the central dip was a Doppler-free saturation dip, rather than just a signal decreasing in a profile combining two separated Doppler broadened spectrum due to forward and backward laser beams. The center of the Doppler-free dip (Lorentzian, from atoms with  $v = 0$ ),  $\omega_0$ , was independent on  $\omega_{\text{shift}}$ , and a sensitive marker for the exact center of the atomic transition. The fitting program is written on ROOT platform (CERN) using the built-in Voigt function.

The frequency uncertainty is estimated by:

$$(\Delta f_{\text{unknown}})^2 = (N \times \Delta f_r)^2 + (\Delta f_o)^2 + (\Delta f_b)^2 . \quad (2)$$

The frequency fluctuation of the stabilized repetition frequency was 4 mHz, so the uncertainty of the absolute

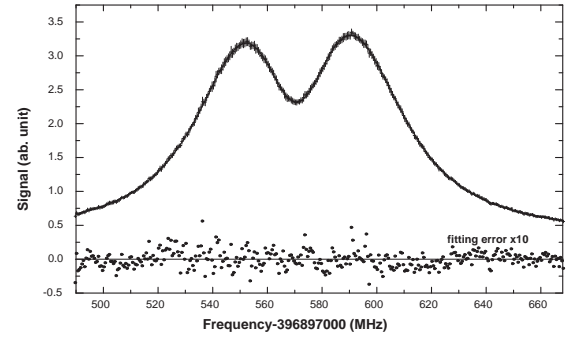


FIG. 6: The histogram of  $^{203}\text{Tl}$   $6P_{1/2} - 7S_{1/2}$  ( $F = 0 \rightarrow F = 1$ ) transition. The frequency axis shown in this figure is the frequency of fundamental laser, not the doubled UV light.

frequency measurement contributed by the first term ( $N \times \Delta f_r$ ) is 2 kHz. The stabilized offset frequency fluctuation  $\Delta f_o$  is only 11 mHz. Therefore, the predominant uncertainty of the absolute frequency measurement in this work is due to the uncertainty of beat frequency,  $\Delta f_b$ , which is the statistic uncertainty from the fitting to histogram data.

### III. RESULTS

#### A. The absolute transition frequency

Figure 6 shows one of transitions with fitting curve, the laser frequency we measured is infrared, rather than atomic transition frequency—UV light. This histogram with 500 kHz binning combined 5 forward-backward scans at different time. The accuracy of measured absolute frequency is sub-MHz, as the signal-to-noise ratio (S/N) is  $\sim 50$ , and the FWHM of Lamb dip is  $< 30$  MHz. The final absolute frequency measurements of all six components of thallium  $6P_{1/2} - 7S_{1/2}$  transitions, including three hyperfine transitions and two isotopes, are listed in Table I. They are labeled as  $A - F$  for identification, and in comparison with the previous experimental measurement and the theoretical calculation.

#### B. HFS, IS and the Mean Square Isotopic Change $\lambda_{c,m}$

Our hyperfine splitting and isotope shift measurements are in good agreement with the previous experimental results as shown in Table II. Our measurement of  $6P_{1/2}$  hyperfine splitting, using purely optical method, is consistent with the magnetic resonance experiment in 1956 [19],

TABLE I: The transition frequencies of  $6P_{1/2} \rightarrow 7S_{1/2}$ .

Line	Transition	Laser frequency (MHz)
A	$^{203}\text{Tl } F=1 \rightarrow 0$	793 761 855.9 (2)
B	$^{205}\text{Tl } F=1 \rightarrow 0$	793 763 376.9 (3)
C	$^{203}\text{Tl } F=1 \rightarrow 1$	793 774 036.3 (3)
D	$^{205}\text{Tl } F=1 \rightarrow 1$	793 775 672.9 (2)
E	$^{203}\text{Tl } F=0 \rightarrow 1$	793 795 141.6 (3)
F	$^{205}\text{Tl } F=0 \rightarrow 1$	793 796 983.4 (5)
Experiment [16]	$6P_{1/2} \rightarrow 7S_{1/2}$	793 775.5 (GHz)
Theory[7]	$6P_{1/2} \rightarrow 7S_{1/2}$	793 100(10) (GHz)

however our result is less accurate. For the  $7S_{1/2}$  hyperfine splitting, our measurement improved the accuracy by a factor of  $7 \sim 8$ , in comparison with the most recent measurements using gas cell [10] and single laser atomic beam [12]. The  $6P_{1/2} \rightarrow 7S_{1/2}$  transition isotope shift between  $^{205}\text{Tl}$  and  $^{203}\text{Tl}$  ( $\delta\nu_{205-203} = 1659.0(6)$  MHz) was also measured. This result is in very agreement with [10].

The hyperfine anomaly,  $\Delta = [(A_{205}/A_{203})(g_{203}/g_{205}) - 1]$ , can be deduced from our measured hyperfine constants  $A_{205}$  and  $A_{203}$ . Using the most precise magnetic moments measured in [22],  $\Delta = -3.34(23) \times 10^{-4}$  was deduced. The hyperfine anomaly can be used to infer a parameter for the mean square isotopic change  $\lambda_{c,m}$  [20], which is related to the magnetic moments and charge distributions in the isotopes. We infer

$$\lambda_{c,m} = 0.44(3) \text{ fm}^2$$

using our experimental results. This parameter inferred from the results of the  $7S_{1/2}$  state HFS reported in [10] is given as  $\lambda_{c,m} = 0.61(20) \text{ fm}^2$  and  $\lambda_{c,m} = 0.45(24) \text{ fm}^2$  in [12].  $\lambda_{c,m} = 0.42 \text{ fm}^2$  can also be given based on much more precise ground state  $^6P_{1/2}$  HFS measured by [20] and [19]. All of these measurements are summarized in Fig. 7. Our result is the most precise value based on  $7S_{1/2}$  HFS.

#### IV. CONCLUSION

The Doppler-free spectroscopy of atomic thallium  $6P_{1/2} \rightarrow 7S_{1/2}$  was observed using atomic beam. For the

first time, the absolute transition frequencies of six components of  $^{203}\text{Tl}$  and  $^{205}\text{Tl}$  were measured to sub-MHz accuracy. These results improve the measurement of hyperfine splittings of  $7S_{1/2}$  state. The mean square isotopic change  $\lambda_{c,m}$  deduced from the hyperfine anomaly of  $7S_{1/2}$  state have also been improved. Our result is in very good agreement with the most precise value from the hyperfine anomaly of  $6P_{1/2}$ .

The optical pumping effect tapping the population on  $6P_{3/2}$  state can be used for the future laser cooling of

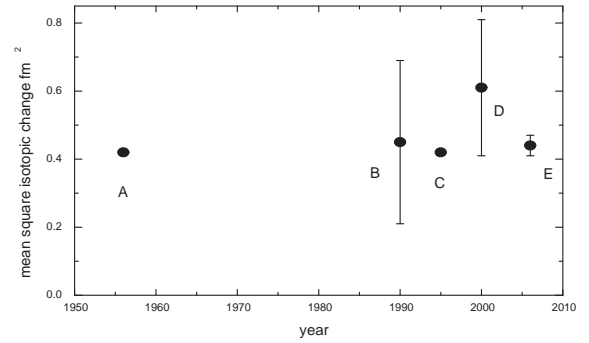


FIG. 7: Comparison of the mean square isotopic change based on various experimental results :

- A. 1956-HFS of  $6P_{1/2}$  ([19])
- B. 1990-HFS of  $7S_{1/2}$  ([12])
- C. 1995-HFS of  $6P_{1/2}$  ([20])
- D. 2000-HFS of  $7S_{1/2}$  ([10])
- E. HFS of  $7S_{1/2}$  (this work)

atomic thallium through  $6P_{3/2} \rightarrow 5D_{5/2}$  transition using a 351 nm laser. Similar cooling schemes have been realized in other atomic species of AIII group [23][24]. Laser cooled atomic thallium beam could further improve various experiments on testing fundamental atomic physics using atomic thallium.

#### Acknowledgments

This work was supported by the National science council of Taiwan under Grant No.95-2112-M-007-005-.

---

- [1] B. C. Regan, E. D. Commins, C. J. Schmidt, and D. De Mille, Phys. Rev. Lett. **88**, 071805 (2002).
- [2] P. A. Vetter, D. M. Meekhof, P. K. Majumder, S. K. Lamoreaux, and E. N. Fortson, Phys. Rev. Lett. **74**, 2658 (1995).
- [3] N. H. Edwards, S. J. Phipp, P. E. G. Baird, and S. Nakayama, Phys. Rev. Lett. **74**, 2654 (1995).
- [4] C. S. Wood, S. C. Bennett, D. Cho, B. P. Masterson, J. L. Roberts, C. E. Tanner, and C. E. Wieman, Science **275**, 1759 (1997).
- [5] M. G. Kozlov, S. G. Porsev, and I. I. Tupitsyn, Phys. Rev. Lett. **86**, 3260 (2001).

TABLE II: Hyperfine splittings and isotope shift (IS). All results are in MHz

	$^{205}\text{Tl}$ 6P <sub>1/2</sub>	$^{203}\text{Tl}$ 6P <sub>1/2</sub>	$^{205}\text{Tl}$ 7S <sub>1/2</sub>	$^{203}\text{Tl}$ 7S <sub>1/2</sub>	IS of 6P <sub>1/2</sub> $\rightarrow$ 7S <sub>1/2</sub>
This work	21310.5(3)	21105.3(3)	12296.0(2)	12180.3(2)	1659.0(6)
Ref.[10]			12294.5(15)	12180.5(18)	1659.0(6)
Ref.[12]			12297.2(16)	12181.6(22)	
Ref.[17]			12284.0(60)	12172.0(60)	
Ref.[18]			12318(36)	12225(42)	
Ref.[19]	21310.835(5)	21105.447(5)			
Theory[7]	21663		12666		
Theory[20]	21300		12760		
Theory[21]	21623		12307		

[6] V. A. Dzuba, C. Harabati, W. R. Johnson, and M. S. Safranova, Phys. Rev. A **63**, 044103 (2001).

[7] M. G. Kozlov, S. G. Porsev, and W. R. Johnson, Phys. Rev. A **64**, 052107 (2001).

[8] V. A. Dzuba, V. V. Flambaum, and M. G. Kozlov, Phys. Rev. A **54**, 3948 (1996).

[9] S. A. Diddams, D. J. Jones, J. Ye, S. T. Cundiff, and J. L. Hall, Phys. Rev. Lett. **84**, 5102 (2000).

[10] D. S. Richardson, R. N. Lyman, and P. K. Majumder, Phys. Rev. A **62**, 012510 (2000).

[11] Y.-W. Liu and P. E. G. Baird, J. Phys. B: At. Mol. Opt. Phys. **35**, 4241 (2002).

[12] G. Hermann, G. Lasnitschka, and D. Spengler, Z. Phys. D **28**, 127 (1993).

[13] W. Demtroder, *Laser spectroscopy : basic concepts and instrumentation* (Springer, New York, 2003), 3rd ed.

[14] B. Couillaud and T. W. Hänsch, Opt. Commun. **35**, 441 (1980).

[15] H.-C. Chui, Ph.D. thesis, National Tsing Hua University (2004).

[16] Kurucz, *Atomic spectral line database from kurucz files*, URL <http://cfa-www.harvard.edu/amdata/amdata/kurucz23/sekur.html>

[17] R. Neugart, Phys. Rev. Lett. **55**, 1559 (1985).

[18] C. Schuler, M. Ciftan, L. B. III, and H. Stroke, J. Opt. Soc. America **52**, 501 (1962).

[19] A. Lurio and A. G. Prodell, Phys. Rev. **101**, 79 (1956).

[20] A.-M. Mårtensson-Pendrill, Phys. Rev. Lett. **74**, 2184 (1995).

[21] V. A. Dzuba, V. V. Flambaum, M. G. Kozlov, and S. G. Porsev, Sov. Phys.-JETP **87**, 885 (1998).

[22] P. Raghavan, At. Data and Nucl. Data Tables **42**, 189 (1989).

[23] R. W. McGowan, D. M. Giltner, and S. A. Lee, Opt. Lett. **20**, 2535 (1995).

[24] S. Rehse, R. McGowan, and S. Lee, Appl. Phys. B **70**, 657 (2000).